

11.10

ANALYSIS OF POLDER POLARIZATION MEASUREMENTS
DURING ASTEX AND EUCREX EXPERIMENTS

Hui Chen, Qingyuan Han*, Joyce Chou and Ronald M. Welch

Institute of Atmospheric Sciences
South Dakota School of Mines and Technology

1. INTRODUCTION

Polarization is more sensitive than intensity to cloud microstructure such as the particle size and shape, and multiple scattering does not wash out features in polarization as effectively as it does in the intensity. Polarization measurements, particularly in the near IR, are potentially a valuable tool for cloud identification and for studies of the microphysics of clouds.

The POLDER instrument is designed to provide wide field of view bidirectional images in polarized light. During the ASTEX-SOFIA campaign on June 12th, 1992, over the Atlantic Ocean (near the Azores Islands), images of homogeneous thick stratocumulus cloud fields were acquired. During the EUCREX'94 (April, 1994) campaign, the POLDER instrument was flying over the region of Brittany (France), taking observations of cirrus clouds.

This study involves model studies and data analysis of POLDER observations. Both models and data analysis show that POLDER can be used to detect cloud thermodynamic phases. Model results show that polarized reflection in the $\lambda = 0.86 \mu\text{m}$ band is sensitive to cloud droplet sizes but not to cloud optical thickness. Comparison between model and data analysis reveals that cloud droplet sizes during ASTEX are about $5 \mu\text{m}$, which agrees very well with the results of *in situ* measurements ($4\text{-}5 \mu\text{m}$). Knowing the retrieved cloud droplet sizes, the total reflected intensity of the POLDER measurements then can be used to retrieve cloud optical thickness. The close agreement between data analysis and model results during ASTEX also suggests the homogeneity of the cloud layer during that campaign.

2. MODEL AND DATA

An adding-doubling radiative transfer model was used to account for the polarization of the light, which is originally developed by Hansen and Travis (Hansen and Travis 1974) and recently modified for our purpose.

Corresponding author address: Q. Han, Institute of Atmospheric Sciences, South Dakota School of Mines and Technology, 501 E. St. Joseph Street, Rapid City, SD 57701-3995.

Consider a plane-parallel atmosphere of optical thickness τ illuminated uniformly from above by a parallel beam of radiation. The incident beam may be described by its Stokes parameters: $F = (I_0, Q_0, U_0, V_0)$, where I_0 is the net flux per unit area of the incident beam, and Q_0, U_0 and V_0 are simply related to the degree of polarization, plane of polarization, and ellipticity of the incident beam (Chandrasekhar, 1960). It is desired to find the Stokes parameters for the light diffusely reflected and transmitted by the atmosphere, i.e., $I_r(t, m, \phi)$ and $I_t(t, m, \phi)$, respectively; here I is a column matrix of four elements. Reflection and transmission matrices R and T are defined as:

$$I_r(0, \mu, \phi) = \mu_0 R(\tau; \mu, \mu_0, \phi - \phi_0) F$$

$$I_t(\tau; \mu, \phi) = \mu_0 T(\tau; \mu, \mu_0, \phi - \phi_0) F$$

and each composed of four rows and four columns. This model can calculate R and T matrices for different cloud properties and thus derive I , which is also measured by POLDER instrument.

The results of the model have been compared with other published polarization calculations and show excellent agreements. Another validation effort of the model calculations is simulating the POLDER image using model results and then comparing it with data images. Under the same solar zenith angle condition, the simulated image agrees well with data images. Figure 1 shows one of these comparisons. Black gaps on the rainbow feature show up on both simulated and real data images of Q component of the polarization reflection.

The dataset used for this study is from an airborne POLDER instrument which uses a matrix array of 288×384 squared CCD (Charge-Coupled Device) detectors with focal length $f = 3.47 \mu\text{m}$. This provides an angular coverage with viewing angles q_v of $\pm 42^\circ$ in the along-track or cross-track direction and $\pm 51^\circ$ in the other direction. From a flight altitude of 5000 m above the cloud top, the field-of-view is approximately $9.3 \times 12.3 \text{ km}$ and the resulting POLDER images are partitioned into 288×384 identical cloud pixels with $32 \times 32 \text{ m}$ spatial resolution. The filter wheel has 10 positions,

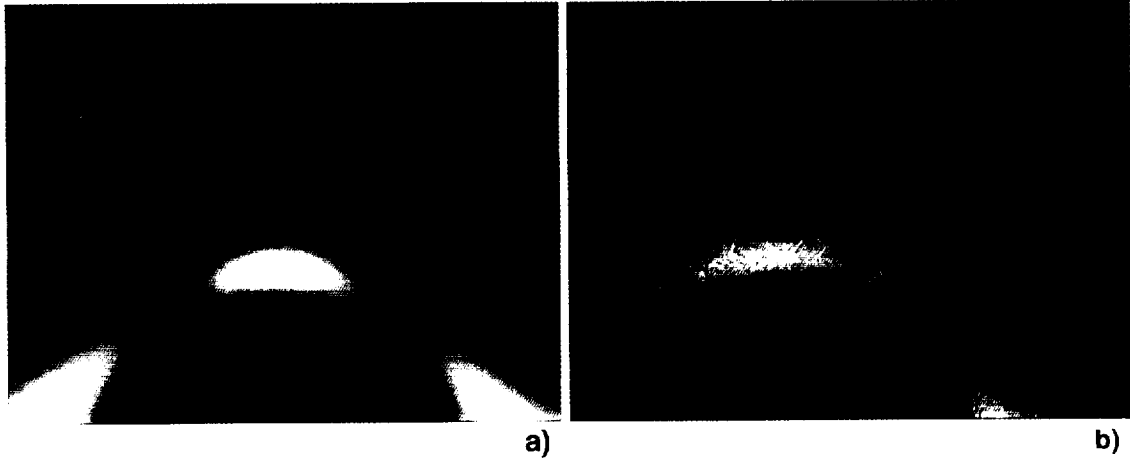


Figure 1. Q component of the polarized reflection, a) model simulated image; b) data image.

including one blind position used for the measurement of the dark current. The system therefore allows measurements in 3 polarized spectral bands, or in 2 polarized and 3 unpolarized bands. A measurement sequence consists in these 9 spectral polarized images plus the darkness current image. The 10 images are acquired in about 3.7 seconds, which is the period of the filter wheel, and the time interval between two consecutive sequences is about 11 seconds (needed for the data transfer to an Exabyte tape recorder). During one full rotation of the filter wheel (10 filters), the displacement is typically 370 m (depending on the aircraft speed), i.e. about 1 or 2 pixels between two successive filters. Finally, the displacement is about 1 km between two consecutive sequences, which allows a surface target to be observed from about 12 different directions (12 successive sequences) as the aircraft flies over.

During the ASTEX-SOFIA campaign on June 12th, 1992, images of homogeneous thick stratocumulus cloud fields were acquired in polarized bands centered at 443 (20nm width) and 865 nm (40 nm width) as well as 3 unpolarized wavelength filters centered on 765 nm, 763 nm and 910 nm. The CCD matrix was oriented along-track. By using pre-flight calibration measurements, the POLDER raw data have been processed and transformed in normalized reflectances, S_{ij}^{ka} , relative to each matrix pixel. The normalized reflectance S_{ij}^{ka} is related to Stokes parameters I , Q , U by $S_{ij}^{ka} = P_i^{ka}I + P_q^{ka}Q + P_u^{ka}U$ where i, j are position indices of a pixel, ka stands for the angle between the meridian plane of the matrix pixel and the first analyzer direction, and P_r, P_q, P_u are coefficients determined by instrument calibration.

The data analysis includes calculating total reflectance, and degree of polarization from

normalized reflectances of the three analyzers at the same wavelength. For each pixel, the angle between the meridian plane and the first analyzer direction has to be determined; the scattering angle has to be calculated according to the solar zenith angle, viewing angle, and relative azimuth angle.

3. CLOUD PHASE DISCRIMINATION

Polarization measurements can be used for discriminating cloud thermodynamic phases. This is based on the rainbow pattern in the polarization reflection which will only appear in spheric particles. Figure 2a (modified from Takano and Liou 1989) shows a model example, which demonstrates the basic principle used for cloud phase detection. Figure

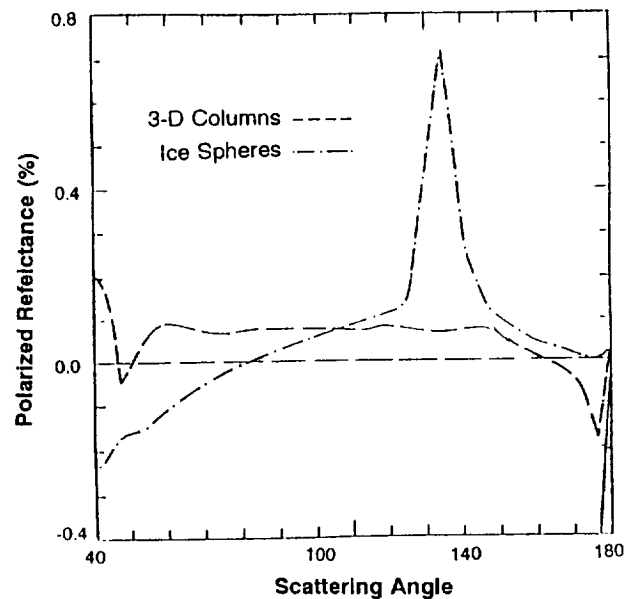


Figure 2a. Cloud particle shape effect on polarized reflectance.

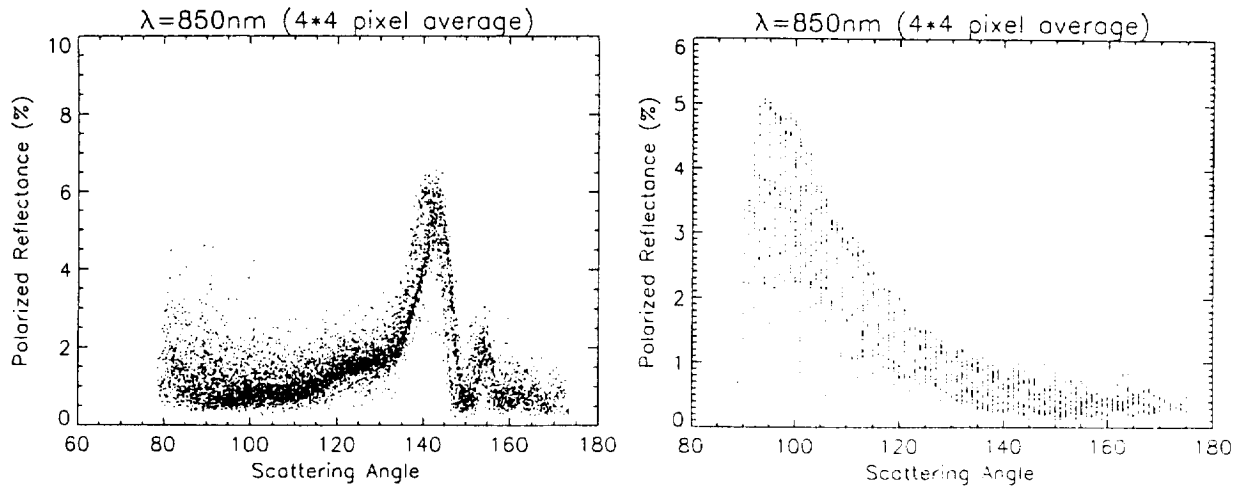


Figure 2b. Observed polarized reflectance from ASTEX (left panel) and EUCREX (right panel).

2b shows two scatter plots taken from ASTEX and EUCREX experiments, respectively. The polarization features around the 140° scattering angle clearly show that the cloud field in ASTEX was water cloud and the cloud from EUCREX was cirrus.

4. CLOUD DROPLET SIZE RETRIEVAL

Some previous studies suggest that polarized reflection from POLDER is not sensitive to cloud drop sizes (Goloub *et al.* 1994). However, this conclusion is drawn from using size distribution parameters not sensitive to scattering cross sections. The present study uses effective radius r_e , defined by Hansen and Travis (1974), to reexamine the sensitivity of polarization to droplet sizes. Figures 3a, 3b show the model results of polarization and total intensity reflection for cloud with optical thickness $\tau=10$, at solar zenith angle $\theta=53^\circ$. These plots suggest that 1) both polarization and total intensity reflections are monotonic functions of r_e ; 2) polarized reflection can be used to estimate cloud droplet sizes if it is not sensitive to cloud optical thickness; and 3) retrieval of cloud optical thickness from total reflected intensity without knowledge of cloud droplet size may cause errors. Figures 4a (for $r_e=5 \mu\text{m}$) and 4b (for $r_e=10 \mu\text{m}$) show that the polarized reflection is not sensitive to cloud optical thickness. Similar conclusion has been reached by Goloub *et al.* (1994).

Comparison between model results (Fig. 4a) and data analysis (Fig. 2b) reveals that the cloud droplet sizes in the ASTEX experiment are around $5 \mu\text{m}$, which agrees well with results from *in situ* aircraft measurements ($4\text{-}5 \mu\text{m}$).

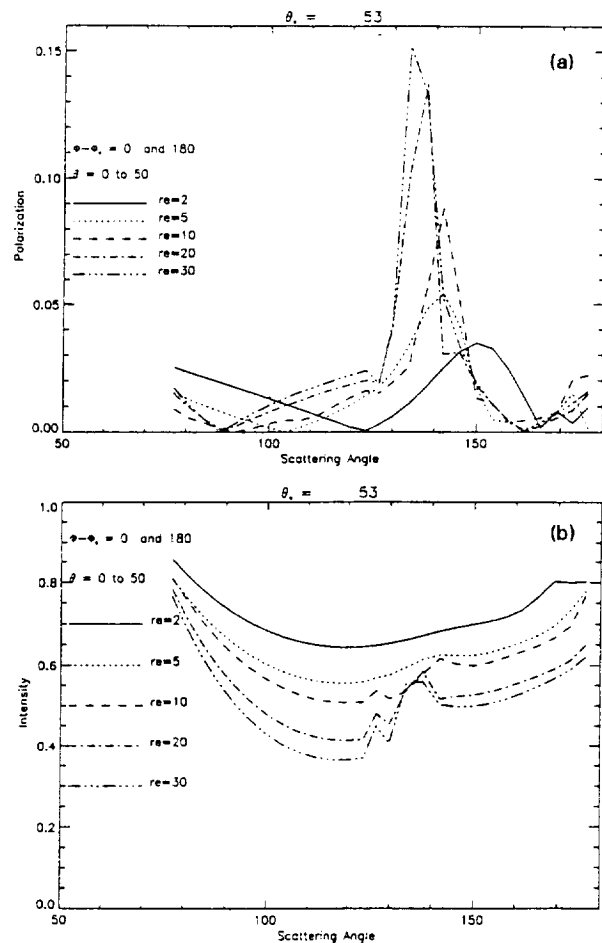


Figure 3. Droplet size effect on polarization (a) and intensity (b).

5. CLOUD OPTICAL THICKNESS

As explained above, with the estimation of cloud droplet size, the result of cloud optical thickness retrieval will be more accurate. Figures 5a and 5b are results from model calculations of total reflected intensity for r_e at different optical thickness values and data analysis from the ASTEX experiment. It seems that cloud optical thicknesses of all pixels are between 10 and 6. Note that the model results are limited to relative azimuth angles $\phi=0^\circ$ and $\phi=180^\circ$, while the results from data analysis are from all azimuth angles. Figure 6 is a simulation of the POLDER image with all azimuth angles using model calculations for $\tau=10$ and $r_e=5 \mu\text{m}$. Comparison between Fig. 5b and Fig. 6 show that most of the scattering range in Fig. 5b can be explained by different azimuth angles with cloud optical thickness $\tau=10$.

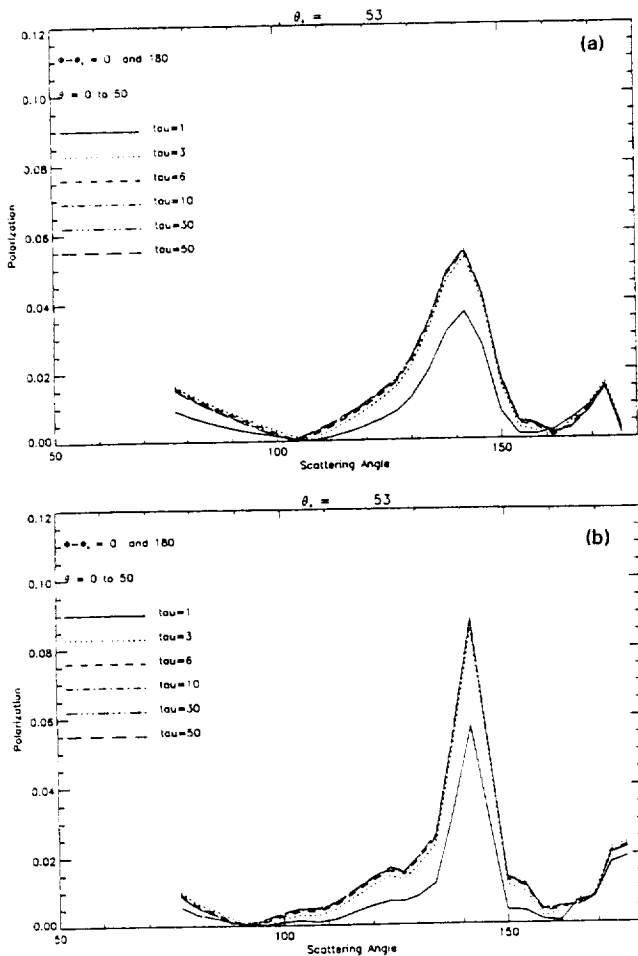


Figure 4. Optical thickness effect on polarization a) $r_e = 5 \mu\text{m}$, b) $r_e = 10 \mu\text{m}$.

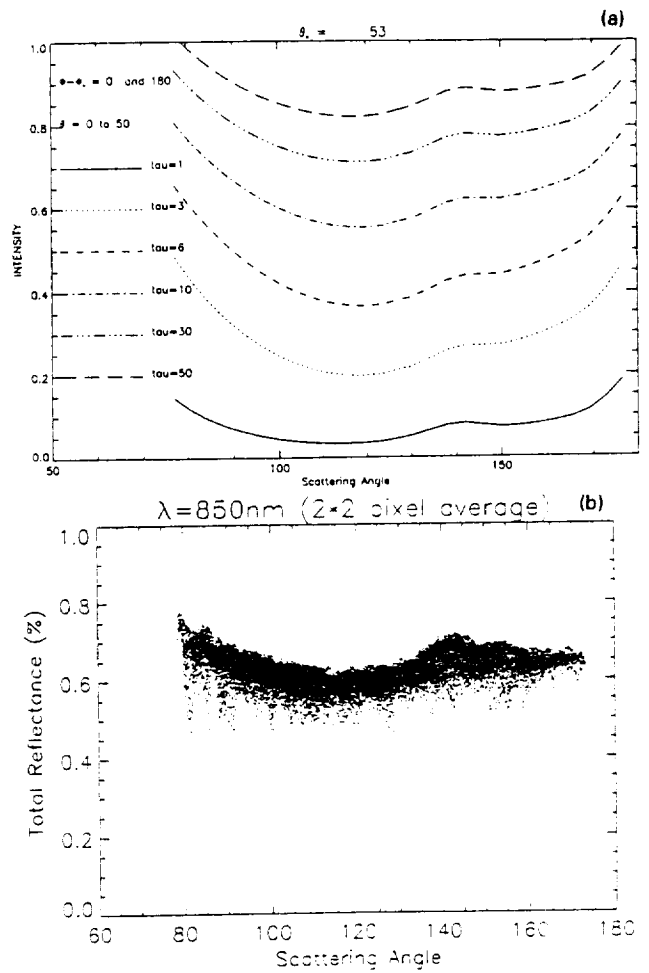


Figure 5 a) Total reflectance for cloud with $r_e = 5 \mu\text{m}$ and different optical thicknesses, b) observed data during ASTEX.

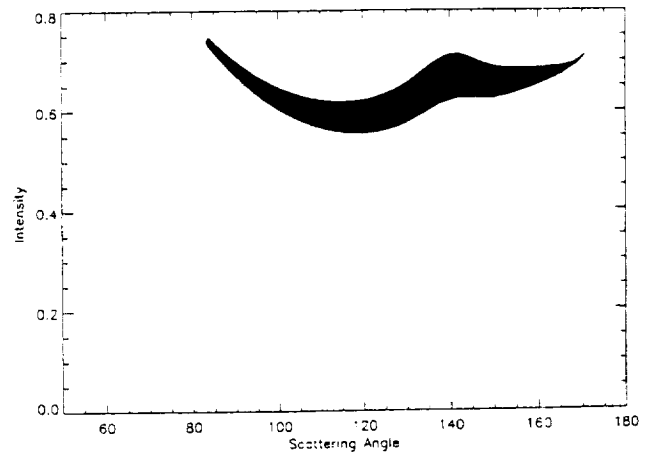


Figure 6. Model simulated image for $\tau=10$ and $r_e = 5 \mu\text{m}$ under the viewing condition of Fig. 5b)

6. SUMMARY

The following are the major conclusions from this study.

1) the POLDER instrument data for stratocumulus and cirrus cloud show distinct cloud phase features.

2) POLDER data can be used to estimate cloud droplet sizes for water clouds. The $\sim 5 \mu\text{m}$ effective droplet radius estimated from POLDER data agrees very well with results from *in situ* aircraft measurement during the ASTEX experiment.

3) Cloud optical thickness can be estimated better with cloud droplet size information derived from POLDER data.

Acknowledgments. This research was supported by NASA contract No. NAS1-19077, NAGW-3788, and NAGW-3922; was partially funded by the U.S. Department of Energy's (DOE) National Institute for Global Environmental Change (NIGEC) through the

NIGEC Great Plains Regional Center at the University of Nebraska-Lincoln (DOE Cooperative Agreement No. DEFC03-90ER61010). Financial support does not constitute an endorsement by DOE of the views expressed in this paper. This research was also supported by the NASA grant NAGW-4791, under Climate Program managed by Dr. Bob Curran.

7. REFERENCES

Hansen, J. E., and L. D. Travis, 1974: Light scattering in planetary atmospheres. *Space Science Review*, **16**, 527-610.

Goloub, P., J. L. Deuze, M. Herman, and Y. Fouquart, 1994: Analysis of the POLDER polarization measurements performed over cloud covers. *IEEE Trans. Geosci. Remote Sensing*, **32**, 78-88.

Takano, Y., and K. N. Liou, 1989: Solar radiative transfer in cirrus clouds. Part II: Theory and computation of multiple scattering in an anisotropic medium. *J. Atmos. Sci.*, **46**, 20-36.

